ORIGINAL ARTICLE / ÖZGÜN MAKALE

DESIGN AND SYNTHESIS OF SOME ARYLHYDRAZONE DERIVATIVES AS POTENTIAL FAAH INHIBITORS

POTANSİYEL FAAH İNHİBİTÖRÜ OLARAK BAZI ARİLHİDRAZON TÜREVİ BİLEŞİKLERİN TASARIMI VE SENTEZİ

Tugce GUR MAZ[1]* iD, Sumeyye TURANLI[1,2] iD, H. Burak CALISKAN[3] iD

[1]Gazi University, Faculty of Pharmacy, Department of Pharmaceutical Chemistry, 06530, Ankara, Turkey

[2]Adıyaman University, Faculty of Pharmacy, Department of Pharmaceutical Chemistry, 02040, Adıyaman, Turkey

[3]TOBB ETU Economy and Technology University, Faculty of Engineering, Department of Biomedical Engineering, 06560, Ankara, Turkey

ABSTRACT

Objective: *The aim was to design, synthesis and investigation of possible interactions in the enzyme active site of a series of arylhydrazone derivatives for the inhibition of the FAAH enzyme."*
Material and Method: *Arylhydrazone derivatives were obtained through the reaction of nicotinic hydrazide or benzohydrazide with appropriate aldehyde derivatives, and the obtained crude product was recrystallized from ethanol. After elucidating chemical structures of the compounds via spectroscopic methods, the inhibitory activities against hFAAH were screened. The results were further supported with molecular modeling studies.*
Result and Discussion: *In this study, a new series of seven arylhydrazone derivatives were screened against hFAAH. 4-phenoxyphenyl bearing derivative **5** was found to inhibit hFAAH 40 % at 10 µM which indicates that newly developed inhibitor could serve as a starting point for improving inhibitory effect of the new series.*
Keywords: *Arylhydrazones, FAAH, heterocycles, inflammation*

ÖZ

Amaç: *FAAH enziminin inhibisyonu amacıyla bir seri arilhidrazon türevi bileşiğin tasarımı, sentezi ve enzim aktif bölgesinde olası etkileşimlerinin incelenmesidir.*

---

* **Corresponding Author / Sorumlu Yazar:** Tugce Gur Maz
  e-mail / e-posta: ztugcegur@gazi.edu.tr, **Phone / Tel.:** +90 312 202 3223

Gereç ve Yöntem: *Nikotinik hidrazit veya benzohidrazidin uygun aldehit türevleri ile reaksiyonu sonucu arilhidrazon türevleri elde edilmiş, elde edilen ham ürünler etanolden rekristalize edilmiştir. Bileşiklerin yapısı spektroskopik yöntemler ile aydınlatıldıktan sonra hFAAH enzimine karşı aktiviteleri taranmıştır. Elde edilen sonuçlar moleküler modelleme çalışmaları ile desteklenmiştir.* **Sonuç ve Tartışma:** *Bu çalışmada, bir seri yedi arilhidrazon türevi hFAAH'a karşı taranmıştır. 4-fenoksifenil içeren türev olan Bileşik **5**'in 10 uM'de hFAAH'ı % 40 oranında inhibe ettiği bulunmuş olup; ileri çalışmalarda potansiyel hFAAH inhibitörü olarak kullanılabilecek yeni bir arilhidrazon türevine ulaşılmıştır.* **Anahtar Kelimeler:** *Arilhidrazonlar, FAAH, heterosiklikler, inflamasyon*

INTRODUCTION

FAAH (Fatty Acid Amide Hydrolase) is a membrane enzyme and a member of serine hydrolase family with a catalytic triad comprising Ser217, Ser 241 and Lys142. FAAH is responsible for the hydrolysis of the endogenous cannabinoid (eCB) anandamide (AEA). The cannabinoid receptors CB1 and CB2 are activated by endogenous lipid endocannabinoids, such as AEA and 2-arachidonylglycerol (2-AG) [1, 2]. The eCB system regulates several physiological processes in the central nervous system (CNS). Disruptions in the eCB have been thought to be linked to several pathological conditions such as neuropsychiatric disorders, inflammation, and pain [2-4]. The altered levels of FAAH have been found in patients suffering from Alzheimer's and Huntington's diseases. Inhibition of FAAH have been observed to induce an increase in the level of endogen AEA and other FAAs, resulting analgesic, antiinflammatory, antidepressant and anxiolytic effects without introducing severe adverse effects which have been seen with direct CB receptor agonists such as cannabis [5]. Pre-clinical significance of FAAH inhibition suggested that FAAH may be an important therapeutic target in the treatment of some neurological disorders [6].

In the past years, different chemotypes possessing many potent FAAH inhibitors have been developed some of which have even carried into clinical trials to assess their potential against anxiety, mood disorders, osteoarthritis and cannabis withdrawal syndrome (Figure 1) [7-9]. Amongst others, the one with **BIA 10-2474** was shown severe adverse effect [10]. Recently, **PF-04457845** was found to be effective in cannabis withdrawal syndrome in a Phase II study [11], however, none of these inhibitors have reached to the market yet.
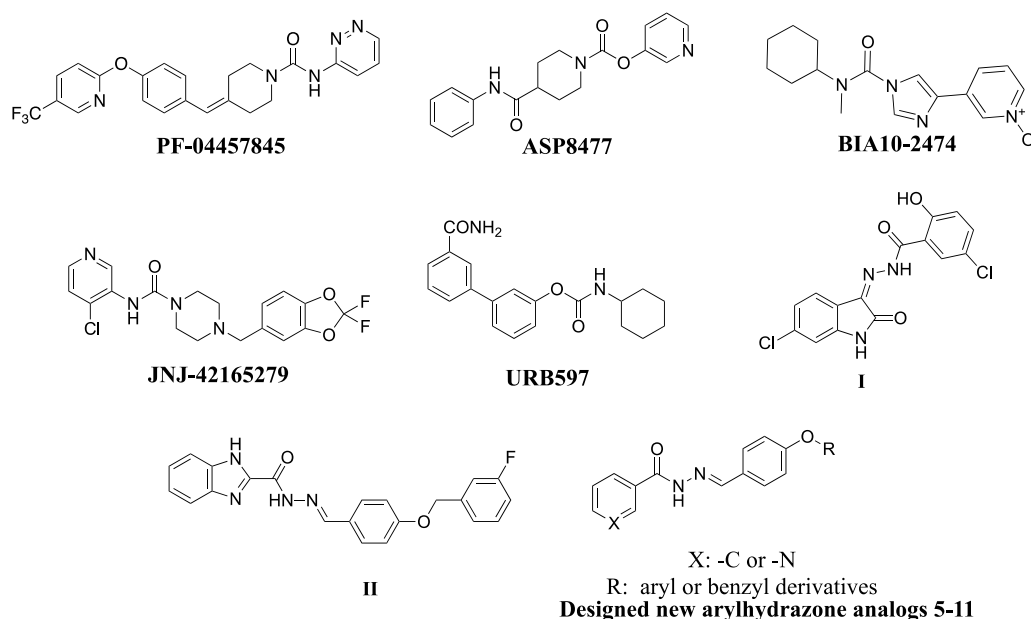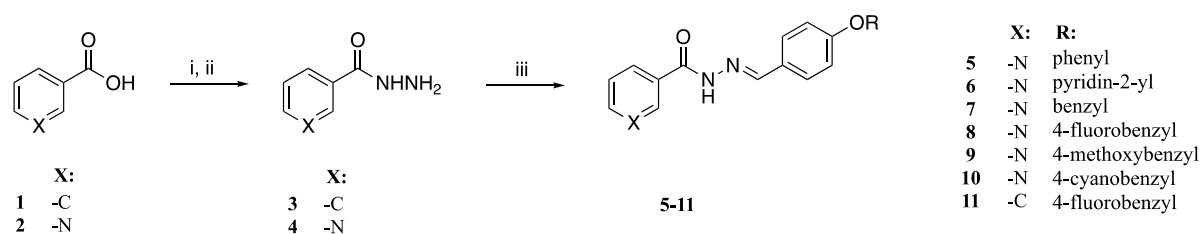

Figure 1. Some known FAAH inhibitors.

Different types of scaffolds have been identified as FAAH inhibitors and yet, mostly, urea and carbamate bearing compounds have been reported [4,11,12]. Recently, carbohydra-zone based **I** and **II** (Figure 1) have been identified as FAAH inhibitors [13,14]. Inspired by the reported compounds in the literature, we aimed to identify potential FAAH inhibitors that might serve as suitable new chemical libraries for further development. Having set this purpose, we designed a small series of arylhydrazone derivatives and evaluated them against human FAAH (hFAAH).

MATERIAL AND METHOD

Chemistry

All starting materials were purchased from Merck. The reactions were verified with TLC using silica gel plates, which were visualized under 254 nm UV light. The NMR spectra of the compounds were recorded on a Varian Mercury 400 MHz or Bruker Avance NEO 500 MHz spectrometers. Final compounds were recrystallized from ethanol. Purity of the compounds were verified by UPLC-MS system interconnecting with time of flight (TOF) in electrospray ionization in ESI (+) mode. Stuart SMP50 melting point apparatus was used for determination of the melting points of the compounds. The chemical structures of the compounds were characterized using ^{1}H-NMR and ^{13}C-NMR spectra which were recorded in DMSO-d_6.

X:	R:
5 -N	phenyl
6 -N	pyridin-2-yl
7 -N	benzyl
8 -N	4-fluorobenzyl
9 -N	4-methoxybenzyl
10 -N	4-cyanobenzyl
11 -C	4-fluorobenzyl

X:		X:		**5-11**
1 -C		**3** -C		
2 -N		**4** -N		

Reagent and conditions: i) MeOH, H_2SO_4, Δ; *ii)* hydrazine hydrate, MeOH, Δ; *iii)* 4-phenoxybenzaldehyde (for **5**); 4-(pyridin-2-yloxy)benzaldehyde (for **6**); 4-(benzyloxy)benzaldehyde (for **7**); 4-(fluorobenzyloxy)benzaldehyde (for **8**); 4-(methoxybenzyloxy)benzaldehyde (for **9**); 4-(cyanobenzyloxy)benzaldehyde (for **10**); 4-(fluorobenzyloxy)benzaldehyde (for **11**); EtOH, Δ, 2h.

Figure 2. Synthetic route of title compounds.

Benzohydrazide (3) and pyridine-3-carbohydrazide (4). To a solution of 1 (3.3 mmol, 1 eq) or 2 (15.1 mmol, 1 eq) were dissolved in EtOH (10 ml), conc. sulfuric acid (3 ml) was added onto it carefully, and the resulting mixture was refluxed overnight. After cooling it to rt, the excess of solvent evaporated. pH was neutralized with NaHCO$_3$ solution, and the precipitated product was filtered and dried to give ethylbenzoate and ethyl pyridine-3-carboxylate, respectively. To a solution of ethylbenzoate and ethyl pyridine-3-carboxylate in EtOH, hydrazine hydrate was added (1.5 eq). The resulting mixture was refluxed overnight. After cooling to RT, the precipitated solid was filtered from EtOH to obtain the crude 3 or 4 which were used without further purification. The data for 3 are as follows: Yield: overall 2 steps, 34.5%. Mp 114.5-116.4ºC, 114-115ºC [15]. The data for 4 are as follows: Yield: overall 2 steps, 29.4%. Mp 150-152ºC, 154-155ºC [16].

General Procedure for the Synthesis of 5-11

To a solution of arylhydrazides (3 or 4) (1 eq) in EtOH, corresponding aldehydes were added and the resulting mixture was refluxed for 2 hours. After cooling to RT, the solution was filtered and recrystallized from ethanol to obtain arylhydrazone derivatives (5-11).

N'-[(E)-(4-phenoxyphenyl)methylidene]pyridine-3-carbohydrazide (5). Yield: 78%. Mp 136.0-138.0ºC. ^{1}H-NMR (500 MHz, DMSO-d_6): δ 7.06-7.12 (4H, m), 7.21 (1H, t, *J* = 7.5 Hz), 7.45 (2H, t, *J* = 8.0 Hz), 7.57 (1H, dd, *J* = 8.0, 5.0 Hz), 7.76 (2H, d, *J* = 9.0 Hz), 8.28 (1H, d, *J* = 8.0 Hz), 8.48 (1H, s), 8.76-8.77 (1H, m), 8.95, 9.09 (1H, d, *J* = 1.5 Hz), 12.07 (1H, s); ^{13}C-NMR (125 MHz, DMSO-d_6): δ

118.7, 119.9, 124.1, 124.7, 129.6, 129.7, 130.7, 135.9, 148.3, 149.1, 152.7, 156.2, 159.2, 162.1. HRMS (m/z) [M+H]$^+$ calculated for $C_{19}H_{16}N_3O_2$: 318.1243; found: 318.1233. CAS # 358767-07-4.

N'-[(E)-[4-(pyridin-2-yloxy)phenyl]methylidene]pyridine-3-carbohydrazide (6). Yield: 47%. Mp 181.2-182.8ºC. ^{1}H-NMR (400 MHz, DMSO-d$_6$): δ 7.10 (1H, d, J = 8.4 Hz), 7.16-7.23 (3H, m), 7.57 (1H, dd, J = 7.6, 5.2 Hz), 7.79 (2H, d, J = 8.8 Hz), 7.87-7.92 (1H, m), 8.13-8.27 (2H, m), 8.47 (1H, s), 8.77 (1H, dd, J = 4.8, 1.2 Hz), 8.95, 9.08 (1H, d, J = 2.0 Hz), 12.0 (1H, s); ^{13}C-NMR (100 MHz, DMSO-d$_6$): δ 112.0, 119.5, 121.4, 123.6, 128.7, 129.2, 130.3, 135.5, 140.4, 147.5, 147.8, 148.6, 152.3, 155.6, 161.6, 162.6. HRMS (m/z) [M+H]$^+$ calculated for $C_{18}H_{15}N_4O_2$: 319.1195; found: 319.1190.

N'-[(E)-[4-(benzyloxy)phenyl]methylidene]pyridine-3-carbohydrazide (7). Yield: 65%. Mp 166.2-167.7ºC. ^{1}H-NMR (500 MHz, DMSO-d$_6$): δ 5.14, 5.17 (2H, 2s), 7.05-7.13 (2H, m), 7.34-7.49 (5H, m), 7.56 (1H, dd, J = 8.0, 5.0 Hz), 7.70 (2H, d, J = 8.5 Hz), 8.26 (1H, dt, J = 8.0, 2.0 Hz), 8.41 (1H, s), 8.76-8.77 (1H, m), 8.95, 9.07 (1H, d, J = 1.5 Hz), 11.8, 11.9 (1H, 2s); ^{13}C-NMR (125 MHz, DMSO-d$_6$): δ 69.8, 115.7, 124.1, 127.4, 128.3, 128.4, 128.9, 129.3, 129.8, 135.9, 137.2, 148.7, 149.0, 152.7, 160.5, 162.0. HRMS (m/z) [M+H]$^+$ calculated for $C_{20}H_{18}N_3O_2$: 332.1399; found: 332.1402. CAS # 292180-66-6.

N'-[(E)-{4-[(4-fluorophenyl)methoxy]phenyl}methylidene]pyridine-3-carbohydrazide (8). Yield: 63%. Mp 182.3-184.2ºC. ^{1}H-NMR (400 MHz, DMSO-d$_6$): δ 5.11, 5.15 (2H, 2s), 7.03-7.12 (2H, m), 7.23 (2H, d, J = 8.8 Hz), 7.48-7.58 (3H, m), 7.70 (2H, d, J = 8.8 Hz), 8.25 (1H, dt, J = 8.0, 2.0 Hz), 8.39 (1H, s), 8.74 (1H, dd, J = 4.8, 1.2 Hz), 8.95, 9.06 (1H, d, J = 1.6 Hz), 11.8, 11.9 (1H, 2s); ^{13}C-NMR (100 MHz, DMSO-d$_6$): δ 68.7, 115.2, 115.3 ($^2J_{C-F}$ = 21.1 Hz), 123.6, 126.9, 128.8, 129.3, 130.0 ($^3J_{C-F}$ = 8.4 Hz), 132.9 ($^4J_{C-F}$ = 2.6 Hz), 135.4, 148.2, 148.5, 152.2, 159.9, 161.5, 161.8 ($^1J_{C-F}$ = 242.4 Hz). HRMS (m/z) [M+H]$^+$ calculated for $C_{20}H_{17}N_3O_2F$: 350.1305; found: 350.1304.

N'-[(E)-{4-[(4-methoxyphenyl)methoxy]phenyl}methylidene]pyridine-3-carbohydrazide (9). Yield: 70%. Mp 201.5-203.4ºC. ^{1}H-NMR (400 MHz, DMSO-d$_6$): δ 3.76 (3H, s), 5.04, 5.08 (2H, 2s), 6.95 (2H, d, J = 8.8 Hz), 7.02-7.10 (2H, m), 7.36-7.41 (2H, m), 7.46-7.57 (1H, m), 7.69 (2H, d, J = 8.4 Hz), 8.25 (2H, dt, J = 8.0, 2.0 Hz), 8.75 (1H, dd, J = 4.8, 1.6 Hz), 8.94, 9.06 (1H, d, J = 1.6 Hz), 11.8, 11.9 (1H, 2s); ^{13}C-NMR (100 MHz, DMSO-d$_6$): δ 55.1, 69.2, 113.8, 115.2, 123.6, 126.7, 128.6, 128.8, 129.3, 129.6, 135.4, 148.3, 148.5, 152.2, 159.1, 160.2, 161.5. HRMS (m/z) [M+H]$^+$ calculated for $C_{21}H_{20}N_3O_3$: 362.1505; found: 362.1504.

N'-[(E)-{4-[(4-cyanophenyl)methoxy]phenyl}methylidene]pyridine-3-carbohydrazide (10). Yield: 79%. Mp 217.8-219.2ºC. ^{1}H-NMR (400 MHz, DMSO-d$_6$): δ 5.25, 5.29 (2H, 2s), 7.04-7.13 (2H, m), 7.48-7.58 (1H, m), 7.62-7.71 (4H, m), 7.88 (2H, d, J = 8.4 Hz), 8.24 (1H, d, J = 8.0 Hz), 8.39 (1H, s), 8.75 (1H, dd, J = 4.8, 1.2 Hz), 8.94, 9.05 (1H, d, J = 1.2 Hz), 11.8, 11.9 (1H, 2s); ^{13}C-NMR (100 MHz, DMSO-d$_6$): δ 63.4, 110.6, 115.2, 118.8, 123.6, 127.2, 128.2, 128.9, 129.3, 132.5, 125.4, 142.6, 148.1, 148.6, 152.2, 159.7, 161.5. HRMS (m/z) [M+H]$^+$ calculated for $C_{21}H_{17}N_4O_2$: 357.1352; found: 357.1336.

N'-[(E)-{4-[(4-fluorophenyl)methoxy]phenyl}methylidene]benzohydrazide (11). Yield: 69%. Mp 212.1-213.8ºC. ^{1}H-NMR (400 MHz, DMSO-d$_6$): δ 5.15, 5.17 (2H, 2s), 7.12 (2H, t, J = 8.8 Hz), 7.22 (2H, t, J = 8.8 Hz), 7.5-7.6 (4H, m), 7.68 (2H, d, J = 8.8 Hz), 7.81 (1H, d, J = 8.8 Hz), 7.91 (2H, d, J = 8.5 Hz), 8.42, 8.62 (1H, 2s), 11.7 (1H, s); ^{13}C-NMR (100 MHz, DMSO-d$_6$): δ 68.6, 115.1, 115.2 ($^2J_{C-F}$ = 21.2 Hz), 126.8, 127.1, 127.4, 128.3, 128.6, 129.8 ($^3J_{C-F}$ = 8.3 Hz), 131.5, 132.9 ($^4J_{C-F}$ = 2.5 Hz), 133.5, 147.6, 159.7, 161.7 ($^1J_{C-F}$ = 241.8 Hz). HRMS (m/z) [M+H]$^+$ calculated for $C_{21}H_{18}FN_2O_2$: 349.1352; found: 349.1346. CAS # 339252-31-2.

Biological Activity

The FAAH assay kit was purchased from Cayman Chemical (Item no: 10005196). The assay protocol was followed to evaluate FAAH inhibition. Briefly, 170 µl of assay buffer (125 mM Tris-HCl, pH 9.0, 1 mM EDTA) was loaded into each well in which 10 µl of inhibitor was then added. Then 10 µl of diluted FAAH enzyme was added to each well and incubated for 5 minutes at 37°C. After incubation, 10 µl of substrate AMC arachidonoyl amide (7-amino-4-methyl coumarin-arachidonamide) was added to start the reaction which was allowed to incubate at 37 °C for 30 minutes. The absorbance of the blank was extracted from initial activity and inhibitor wells. Calculation of the percent inhibition for each compound was done as stated below:

$$\text{İnhibition } \% = [(\text{Initial activity-sample})/\text{Initial activity}] \times 100$$

Molecular Modeling

The X-ray structure of ligand bound FAAH was loaded from the Protein Data Bank (ID 3QK5). The solvent molecules were retained and the protein was preprocessed, optimized and minimized at pH 7.4 using OPLS4 force field in the Schrödinger Protein Preparation Wizard. The grid was positioned at the centre of the bound ligand, and generated using Glide's Receptor Grid Generation module without changing built-in settings. The ligand molecules were prepared using the LigPrep at pH 7.4. Ligand docking was then run with a scaling factor of van der Waals radii 0.90. Only trans conformations were allowed for amides in bias sampling. Strain correction terms were applied for the final output.

RESULT AND DISCUSSION

Chemistry

The synthesis of compounds was accomplished according to the synthetic sequence as demonstrated in Figure 2. In the first step, carboxylic acid derivatives (**1-2**) were reacted with hydrazine hydrate in ethanol to give arylhydrazides (**3-4**) which were converted into corresponding arylhyrazone derivatives (**5-11**) by reacting commercial aldehyde derivatives which were recrystallized from ethanol, then. ^{1}H-NMR and ^{13}C-NMR spectra of the compounds were recorded in DMSO-d_6. Arylhdyrazones are suggested to have four possible isomers in DMSO-d_6. The two derive from geometrical isomers in respect to C=N double bond, and the other two as *syn/antiperiplanar* conformers around the amide CO-NH bond. N-acylhydrazones derived from aromatic aldehydes in solution are anticipated to be in the $E_{C=N}$ form because $Z_{C=N}$ isomer is not observed due to steric hindrance in hydrazones of aldehydes [17-19]. Also, NH signals of $Z_{C=N}$ isomer of arylhyrazones are reported at around 14 ppm [20].

2 singlet signals indicating imino hydrogen (CH=N) were observed at 9.09-8.62 and 8.95-8.42 ppm; the *syn/anti* methylene protons (CH$_2$CO) were also observed typically as 2 singlet signals at 5.07-5.29 and 5.11-5.25 ppm, respectively, all compounds favoring E isomer in DMSO-d_6. The two sets of isomers that belong to methyliden protons (N=CH) and NH protons of the hydrazide is well resolved in **5-11** (Table 1). According to the literature, the most stable isomers are E form in respect to C=N bond and *antiperiplanar* conformer around the CO-NH bond. The CO-NH protons of *anti* conformer was resonated as broad singlets at around 11.9 ppm downfield area whilst *syn* conformer was around at about 11.8 ppm. *Antiperiplanar* conformers were dominant over synplanar form as suggested by the literature. The N=CH proton of carbohydrazide moiety was resonated at about 9.09 ppm for the *antiperiplanar* form while *syn* form was appeared at about 8.94 ppm (Figure 3). Methylene protons belonging to **7-11** were resonated as two singlets at 5.15 and 5.17 ppm.
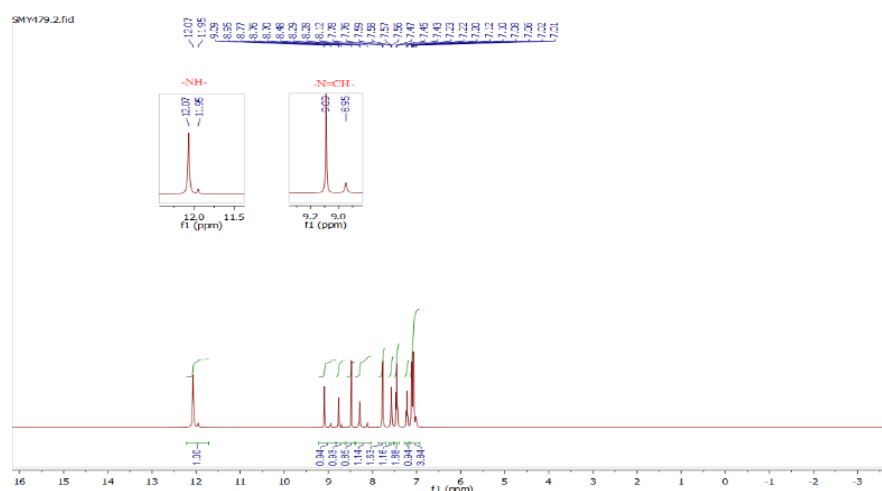

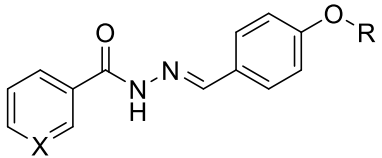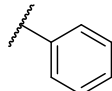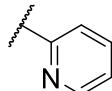**Figure 3.** Representative ^{1}H-NMR spectra of **5**.
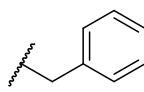
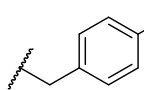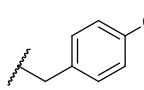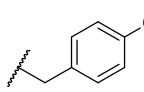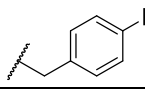The intensity of the peaks allowed us to quantify the ratio of the conformers. The integral intensities of C=NH allowed us to quantify the ratio of the conformers (*anti/syn*) as demonstrated in Table 1. The calculations were revealed that these compounds contained *anti/syn* conformers in a ratio of 85:15 approximately, except compound **11.**

Table 1. Ratio of conformers in DMSO-d_6*

Compound	*anti conformer*	*syn conformer*	*Isomeric Ratio*
	ppm	*ppm*	
5	9.09	8.95	80.6:19.4
6	9.06	8.95	87.7:12.3
7	9.07	8.95	84.7:12.3
8	9.06	8.93	88.2:11.8
9	9.07	8.94	87.9:12.1
10	9.06	8.94	86.4:13.6
11	8.62	8.42	21.5:78.5

* calculated from relative integration of N=CH proton.

Table 2. % FAAH inhibition of arylhydrazones (**5-11**).

#	-X	-R	10 μM	1 μM
5	- N		**40.4**	23.7
6	- N		**37.8**	25.4
7	- N		12.3	2.8
8	- N		N.I	N.I
9	- N		2.1	2.2
10	- N		**32.7**	24.1
11	- CH		5.5	N.I

N.I: no inhibiton

Biological Activity

The compounds were tested against hFAAH at 10 µM and 1 µM, respectively (Table 2). Compounds **5-6**, which were derived from nicotinic hydrazide, were found to inhibit hFAAH at 10 µM about 40%. An additional methylene linkage between aryloxy and phenyl fragments were caused decrease in inhibitory effect of **7-9** while remaining activity in **10** which could be explained by the different electronic properties of the substituents. These findings suggest that the newly identified inhibitors may be used as a starting point for the development of more potent inhibitors.

Molecular Modeling

Molecular docking of the compounds was carried out as described in the Material and Method section. Briefly, an X-ray crystal image with a bound ligand from the PDB (ID:3QK5) was uploaded in the Schrödinger Maestro Docking Suite. The docking parameters were then optimized by docking the X-ray ligand into the active site of the FAAH until the parameters yield a superposition of the ligand. The docking results of binding interactions of three compounds (**5-6** and **10**) show considerable agreement with their activities. In other words, the inhibitory activities of the compounds (40.4% inhibition for **5**, 37.8% inhibition for compound **6** and 32.7% inhibition for **10**) could be explained with binding interactions as revealed in their docking poses (Figure 4-5).
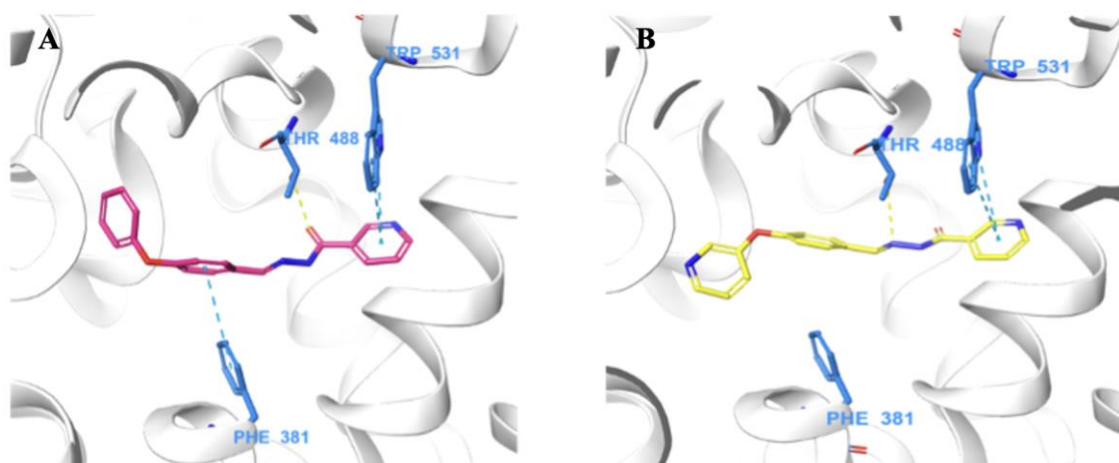

Figure 4. Predicted binding modes of **5** (A) and **6** (B) in the active site of hFAAH (PDB ID: 3QK5)
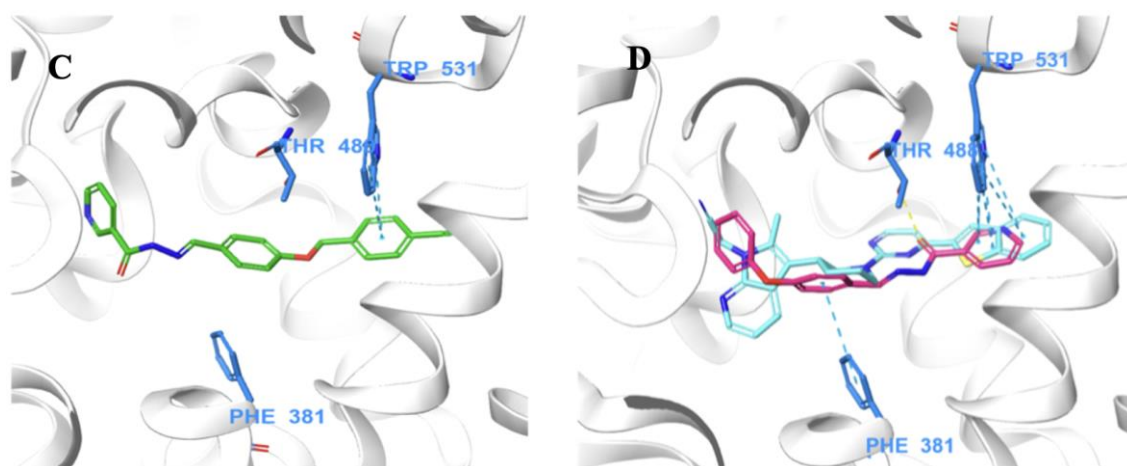

Figure 5. Predicted binding modes of **10** (C) and superposition of **5** with the crystal ligand (D) (PDB ID: 3QK5)

More specifically, compound **5** was found to interact with TRP531 via two π-π stacking bonds, with THR488 via a hydrogen bond and with PHE381 via a π-π stacking bond. Because the molecular structures differ only with the replacement of a carbon atom with a nitrogen in compound **6**, binding modes of compound **6** and compound **5** are similar. Whereas compound **5** binds to THR488 through its oxygen atom, compound **6** makes the same interaction with THR488 via its nitrogen. The difference between binding modes and hence, probably, activities may arise from the lack of π-π stacking with PHE381 in **6**. With respect to **10**, as opposed to **5** and compound **6**, it binds to the TRP531 with two π-π stacking bonds, lacking both the THR488 and PHE381 interactions. This could contribute to the lower activity of **10** compared to either **5** or compound **6** (Figure 5). The highest activity of **5** might be explained through its interactions with three residues, while the second highest activity may reflect the fact that **6** interacts with two residues and the compound with the lowest activity, that is **10**, interacts with only a single residue. However, it should be noted that the number of interactions is not the only factor that contributes to the activity. For instance, the X-ray crystal ligand interacts only with TRP531 through four π-π stacking bonds. Four bonds in total are expected to contribute to the activity of the ligand and yet high inhibition potential most probably arises from the efficient blocking of the active site to be biologically relevant. The molecules in this work also hint the same line of reasoning. The binding mode of **10** is broadly different compared to either **5** or **6** as there is no interaction towards the active site which is thought to be related with its lowest activity.

ACKNOWLEDGEMENTS

AUTHOR CONTRIBUTIONS

Concept: T.G.M., S.T., H.B.C.; Design: T.G.M., S.T, H.B.C.; Control: T.G.M.; Sources: T.G.M.; Materials: T.G.M., S.T., H.B.C.; Data Collection and/or Processing: T.G.M., S.T., H.B.C.; Analysis and/or Interpretation: T.G.M., S.T., H.B.C.; Literature Review: T.G.M., S.T., H.B.C.; Manuscript writing: T.G.M., S.T., H.B.C.; Critical Review: T.G.M., S.T., H.B.C.; Other: -

CONFLICT OF INTEREST

The authors declare that there is no real, potential, or perceived conflict of interest for this article.

ETHICS COMMITTEE APPROVAL

The authors declare that the ethics committee approval is not required for this research.

REFERENCES

1.   Van Egmond, N., Straub, V.M., van der Stelt, M. (2021). Targeting Endocannabinoid Signaling: FAAH and MAG Lipase Inhibitors. Annual Review of Pharmacology and Toxicology, 61, 441-463. [CrossRef]
2.   Mechoulam, R., Parker, L. A. (2013). The Endocannabinoid System and the Annual Review of Psychology, 64(1), 21-47. [CrossRef]
3.   Lutz, B., Marsicano, G., Maldonado, R., Hillard, C.J. (2015). The endocannabinoid system in guarding against fear, anxiety and stress. Nature Reviews Neuroscience, 16(12), 705-718. [CrossRef]
4.   Tuo, W., Leleu-Chavain, N., Spencer, J., Sansook, S., Millet, R., Chavatte, P. (2017). Therapeutic Potential of Fatty Acid Amide Hydrolase, Monoacylglycerol Lipase, and N-Acylethanolamine Acid Amidase Inhibitors. Journal of Medicinal Chemistry, 60(1), 4-46. [CrossRef]
5.   Sachs, J., McGlade, E., Yurgelun-Todd, D. (2015). Safety and Toxicology of Cannabinoids. Neurotherapeutics, 12(4), 735-746. [CrossRef]
6.   Bajaj, S., Jain, S., Vyas, P., Bawa, S., Vohora, D. (2021). The role of endocannabinoid pathway in the neuropathology of Alzheimer's disease: Can the inhibitors of MAGL and FAAH prove to be potential

therapeutic targets against the cognitive impairment associated with Alzheimer's disease? Brain Research Bulletin, 174, 305-322. [CrossRef]

7.   Bonifácio, M.J., Sousa, F., Aires, C., Loureiro, A.I., Fernandes-Lopes, C., Pires, N.M., Palma, P.N., Moser, P., Soares-da-Silva, P. (2020). Preclinical pharmacological evaluation of the fatty acid amide hydrolase inhibitor BIA 10-2474. British Journal of Pharmacology, 177(9), 2123-2142. [CrossRef]

8.   Ahn, K., Smith, S.E., Liimatta, M.B., Beidler, D., Sadagopan, N., Dudley, D.T., Young, T., Wren, P., Zhang, Y., Swaney, S., Van Becelaere, K., Blankman, J.L., Nomura, D.K., Bhattachar, S.N., Stiff, C., Nomanbhoy, T.K., Weerapana, E., Johnson, D.S., Cravatt, B.F. (2011). Mechanistic and pharmacological characterization of PF-04457845: a highly potent and selective fatty acid amide hydrolase inhibitor that reduces inflammatory and noninflammatory pain. The Journal of Pharmacology and Experimental Therapeutics, 338(1), 114-124. [CrossRef]

9.   Ahn, K., Johnson, D.S., Mileni, M., Beidler, D., Long, J.Z., McKinney, M.K., Weerapana, E., Sadagopan, N., Liimatta, M., Smith, S. E., Lazerwith, S., Stiff, C., Kamtekar, S., Bhattacharya, K., Zhang, Y., Swaney, S., Van Becelaere, K., Stevens, R.C., Cravatt, B.F. (2009). Discovery and characterization of a highly selective FAAH inhibitor that reduces inflammatory pain. Chemistry & Biology, 16(4), 411-420. [CrossRef]

10. Rocha, J.F., Santos, A., Gama, H., Moser, P., Falcao, A., Pressman, P., Wallace Hayes, A., Soares-da-Silva, P. (2022). Safety, Tolerability, and Pharmacokinetics of FAAH Inhibitor BIA 10-2474: A Double-Blind, Randomized, Placebo-Controlled Study in Healthy Volunteers. Clinical Pharmacology & Therapeutics, 111(2), 391-403. [CrossRef]

11. Tripathi, R.K.P. (2020). A perspective review on fatty acid amide hydrolase (FAAH) inhibitors as potential therapeutic agents. European Journal of Medicinal Chemistry, 188, 111953. [CrossRef]

12. Fazio, D., Criscuolo, E., Piccoli, A., Barboni, B., Fezza, F., Maccarrone, M. (2020). Advances in the discovery of fatty acid amide hydrolase inhibitors: what does the future hold? Expert Opinion on Drug Discovery, 15(7), 765-778. [CrossRef]

13. Shang, Y., Hao, Q., Jiang, K., He, M., Wang, J. (2020). Discovery of heterocyclic carbohydrazide derivatives as novel selective fatty acid amide hydrolase inhibitors: design, synthesis and anti-neuroinflammatory evaluation. Bioorganic Medicinal Chemistry Letters, 30(10), 127118. [CrossRef]

14. Jaiswal, S., Ayyannan, S.R. (2022). Discovery of Isatin-Based Carbohydrazones as Potential Dual Inhibitors of Fatty Acid Amide Hydrolase and Monoacylglycerol Lipase. ChemMedChem, 17(1), e202100559. [CrossRef]

15. Freitas, R., Barbosa, J.M.C., Bernardino, P., Sueth-Santiago, V., Wardell, S., Wardell, J.L., Decote-Ricardo, D., Melo, T. G., da Silva, E.F., Salomao, K., Fraga, C.A.M. (2020). Synthesis and trypanocidal activity of novel pyridinyl-1,3,4-thiadiazole derivatives. Biomedicine & Pharmacotherapy, 127, 110162. [CrossRef]

16. Fugard, A.J., Thompson, B.K., Slawin, A.M., Taylor, J.E., Smith, A.D. (2015). Organocatalytic Synthesis of Fused Bicyclic 2,3-Dihydro-1,3,4-oxadiazoles through an Intramolecular Cascade Cyclization. Organic Letters, 17(23), 5824-5827. [CrossRef]

17. Sarıgöl, D., Yüksel, D., Okay, G., Uzgören-Baran, A. (2015). Synthesis and structural studies of acyl hydrazone derivatives having tetrahydrocarbazole moiety. Journal of Molecular Structure, 1086, 146-152. [CrossRef]

18. Syakaev, V.V., Podyachev, S.N., Buzykin, B.I., Latypov, S.K., Habicher, W.D., Konovalov, A.I. (2006). NMR study of conformation and isomerization of aryl- and heteroarylaldehyde 4-tert-butylphenoxyacetylhydrazones. Journal of Molecular Structure, 788(1-3), 55-62. [CrossRef]

19. Alp, A.S., Kilcigil, G., Ozdamar, E.D., Coban, T., Eke, B. (2005). Synthesis and evaluation of antioxidant activities of novel 1,3,4-oxadiazole and imine containing 1H-benzimidazoles. Turkish Journal of Chemistry, 39, 42-53. [CrossRef]

20. Munir, R., Javid, N., Zia-Ur-Rehman, M., Zaheer, M., Huma, R., Roohi, A., Athar, M.M. (2021). Synthesis of Novel N-Acylhydrazones and Their C-N/N-N Bond Conformational Characterization by NMR Spectroscopy. Molecules, 26(16), 4918. [CrossRef]